

Chain Packing and Dynamics in Polycarbonate Block Copolymers

Christopher A. Klug,^{†,‡} Jinhua Wu,[§] Chaodong Xiao,[§] Albert F. Yee,[§] and Jacob Schaefer^{*,†}

Department of Chemistry, Washington University, St. Louis, Missouri 63130, and Department of Materials Science and Engineering, The University of Michigan, Ann Arbor, Michigan 48109

Received May 6, 1997; Revised Manuscript Received July 9, 1997[®]

ABSTRACT: Dynamic mechanical-loss spectra at 1 Hz, and dipolar rotational spin-echo ¹³C NMR spectra at 15.1 MHz, have been obtained for a series of copolymers of polycarbonate made from monodisperse oligomers of Bisphenol A polycarbonate (B_X), alternating (*via* connecting carbonate linkages) with single units of 3,3',5,5'-tetramethylbisphenol A (T). The mechanical-loss relaxation of B_XT suggests cooperative motions in the copolymer glass at *T* = −100 and −20 °C. The NMR results indicate that no phenylene rings undergo π flips in T units and that most but not all of the B rings flip faster than 10 kHz at 300 K. A necessary but not sufficient condition to constrain a B ring from flipping in B_XT is the presence of both interchain and intrachain T-unit nearest neighbors. These results are interpreted in terms of a packing model for polycarbonate-like systems that emphasizes the importance for chain dynamics of the proximity and cooperative motion of nearest-neighbor chains having similar local orientational order.

Introduction

A continuing goal in the design of engineering plastics is the creation of materials with high ductility, a high glass transition temperature, and a low physical aging rate. Polycarbonate is well-known for its high ductility and low brittle–ductile transition temperature but has the disadvantage of aging rapidly;¹ that is, the ductility of polycarbonate decreases significantly with time under annealing at *T* < *T*_g. We have synthesized a series of polycarbonate copolymers consisting of monodisperse oligomers of Bisphenol A polycarbonate (B_X), alternating (*via* connecting carbonate linkages) with single units of 3,3',5,5'-tetramethylbisphenol A (T). The resulting B_XT copolymers (*X* = 1, 3, 5, 7, 9) permit a systematic variation of engineering mechanical properties,² with an ultimate goal of identification of the molecular properties that polymer glasses must have for both high ductility and slow aging.

A first step toward the understanding of macroscopic properties on a microscopic basis is achieved by monitoring chain motions by both by dynamic mechanical spectroscopy (DMS) and solid-state ¹³C NMR. DMS identifies the presence of sub-*T*_g motions essential for macroscopic relaxation,³ and details of the microscopic nature of this relaxation are inferred from NMR. For example, the ductility of polycarbonate has been related to a pronounced DMS γ relaxation.⁴ This process is believed to involve cooperative chain rearrangements that alter the local volume or shape of the glass and so can relieve stress concentrations quickly.⁵ In addition, similar thermally activated cooperative chain rearrangements have been suggested to gate large-amplitude motions of the polycarbonate phenylene rings,⁶ in particular the so-called ring π flips. Ring flips have been detected in the past by quadrupolar,⁷ chemical-shift,⁸ and dipolar line shapes,⁹ in solid-state ²H, ¹³C, and ¹H–¹³C NMR experiments, respectively. Ring flips are

sensitive to local, mechanically active volume fluctuations in the glass¹⁰ and are suppressed by the more dense chain packing of polycarbonates under high hydrostatic pressure¹¹ or during cold drawing.¹² Thus, the ring flips monitor microscopic events in the glass that are directly related to ductility. In this paper, we report the effects of B_XT chain structure on local packing and motion in the glass by comparisons of the results of DMS and ¹H–¹³C NMR experiments.

Experiments

Synthesis of B_XT Copolymers. Polycarbonate copolymers (B_XT) used in this study had monodispersed B_X block lengths.¹³ The precursor oligomers of narrow length dispersity were made by first protecting one of the two phenolic hydroxyl groups of Bisphenol A by benzylcarbonate to form Bisphenol A benzylcarbonate (Cbz-BPA). This step was followed by reaction of Cbz-BPA with Bisphenol A bis(chloroformate) (in a 2:1 molar ratio) to form the oligomer (B₃) with both chain ends capped by benzylcarbonate. The protecting groups were then removed by hydrogenation with 5% Pd/C as catalyst at room temperature. Oligomers with longer block lengths were produced by repeating the above procedures so that each time two more Bisphenol A repeat units were added. The polydispersity of the oligomers (*M*_w/*M*_n) was 1.08–1.14, as determined by GPC. Polycarbonate B_XT copolymers were synthesized by the copolymerization of the B_X oligomers with tetramethylbisphenol A bis(chloroformate) using the method described by Xiao and Yee.¹³

Sample Preparation for DMS and NMR. Solution-cast thin films were used in the DMS measurements. Homogeneous blends of one part B and one part T (B + T) and of one part BT and six parts T (BT + 6T) were made by precipitation from chloroform into methanol.¹⁴

DMS. Experimental procedures for the DMS tests are described in detail elsewhere.¹⁵

NMR. ¹³C NMR spectra were obtained at room temperature at 15.1 MHz using a 12-in. resistive magnet and a home-built spectrometer, the details of which have been described previously.⁹ The single, 11-mm diameter, radio-frequency coil was connected by a low-loss transmission line to a double-resonance tuning circuit. A 1-kW ENI LPI-10H amplifier was used for the ¹H channel and an ENI A-300 amplifier for the ¹³C channel. Cross-polarization transfers were performed at 50 kHz, carbon π pulses at 50 kHz, and proton dipolar decoupling at 100 kHz. Rotors with 600-mg sample capacities were made from plastic (Kel-F) and supported at both ends by air-pumped journal

[†] Washington University.

[‡] Present address: Department of Chemical Engineering, Stanford University, Stanford, CA 94305.

[§] The University of Michigan.

[®] Abstract published in *Advance ACS Abstracts*, September 1, 1997.

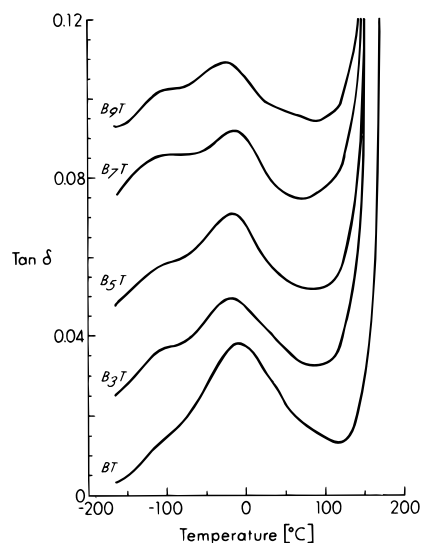


Figure 1. Dynamic mechanical spectra at 1 Hz of a series of B_xT copolymers. Vertical displays have been offset for clarity.

bearings. In these experiments, a 350-mg sample was positioned in the center of the rotor by Kel-F spacers.

DRSE. Carbon dipolar line shapes were characterized by dipolar rotational spin-echo (DRSE) ¹³C NMR extended over one⁹ or two rotor cycles.¹⁶ This is a two-dimensional experiment in which, during the additional time dimension, carbon magnetization is allowed to evolve under the influence of ¹H–¹³C coupling, while ¹H–¹H coupling is suppressed by homonuclear multiple-pulse semi-windowless MREV-8 decoupling.¹⁷ The cycle time for the homonuclear decoupling pulse sequence was 33.6 μs, resulting in decoupling of proton–proton interactions as large as 60 kHz. Sixteen MREV-8 cycles fit exactly into one rotor period with magic-angle spinning at 1859 Hz. A 16-point Fourier transform of the time dependence of the intensity of any peak resolved by magic-angle spinning yields a 16-point dipolar frequency spectrum, scaled by the MREV-8 decoupling and broken up into sidebands by the spinning. Broad dipolar powder spectra (called Pake patterns) appear for carbons with strong ¹H–¹³C coupling, with narrower patterns observed for carbons with weaker couplings. Because the second spinning sideband is near the maximum of a rigid-lattice dipolar Pake powder pattern under the conditions of our experiments,⁹ the ratio of intensities of the second to first dipolar sidebands (*n*₂/*n*₁) is a sensitive measure of averaging of the phenylene-ring ¹H–¹³C dipolar coupling by molecular motion. This ratio changes from about 1.3 in the absence of motion to 0.5 in the presence of large-amplitude motions like ring flips. For example, for the protonated aromatic-carbon peak of the static ring of polycrystalline dimethoxybenzene,¹⁸ we observed an *n*₂/*n*₁ of 1.33, and for the corresponding peak of polycarbonate, we had a value of 0.45. In polycarbonate, the averaging is known⁹ to be dominated by ring flips with flip angles of 180° (or within a few degrees of 180°)¹² occurring at a rate faster than 10 kHz at 300 K. The dipolar sideband *n*₂/*n*₁ intensity ratio is also about 0.5 for a methyl carbon directly bonded to three protons which are undergoing rapid rotations about the methyl-carbon C₃ axis. The DRSE experiment was calibrated by matching the calculated C–H dipolar sideband spectrum (with a room-temperature MREV-8 scale factor¹⁹ of 0.39) for polycrystalline 1,4-dimethoxybenzene.

Results

The 1-Hz DMS spectra of five B_xT copolymers are shown in Figure 1. Distinct γ and β relaxation peaks are observed at −100 and −20 °C, respectively, for all five copolymers. The β peak of B₉T is about half the intensity of that of BT, while the γ peaks appear to be about equal in intensity.

The 15.1-MHz ¹³C NMR spectra of homopolymer B, homopolymer T, and the B + T homogeneous blend²⁰

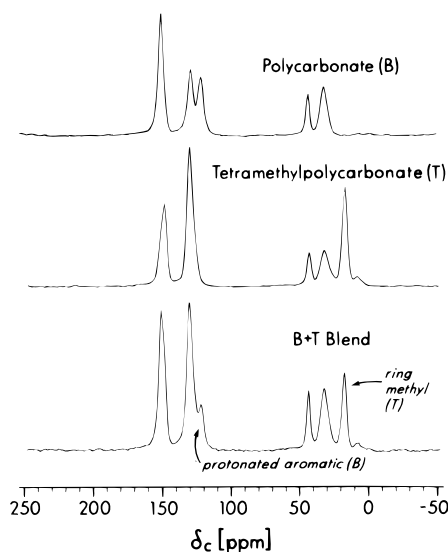


Figure 2. Cross-polarization magic-angle spinning 15.1-MHz ¹³C NMR spectra of polycarbonate (top), tetramethylpolycarbonate (middle), and a homogeneous blend of one part polycarbonate and one part tetramethylpolycarbonate (bottom). Chemical shifts were measured in ppm from external tetramethylsilane.

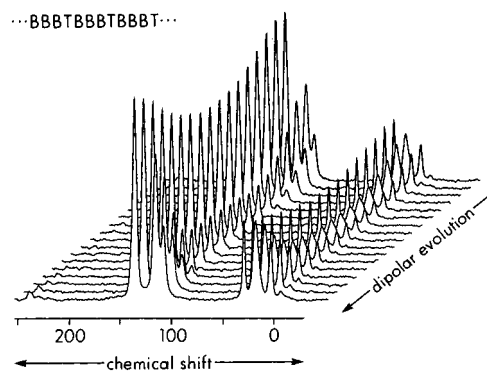


Figure 3. Dipolar rotational spin-echo 15.1-MHz ¹³C NMR spectra of B₃T as a function of the ¹H–¹³C dipolar evolution time during which proton–proton interactions are suppressed by multiple-pulse decoupling. Evolution time with proton–proton interactions suppressed by multiple-pulse decoupling varied from zero to one rotor period. Magic-angle spinning was at 1859 Hz.

show that the protonated aromatic-carbon B peak at 120 ppm and the ring methyl-carbon T peak at 15 ppm are resolved (Figure 2). These carbon signals report the respective ring dynamics of the two components of B_xT copolymers in DRSE experiments. For example, the 120-ppm peak is mostly dephased (but is not inverted) after four MREV-8 cycles, whereas the 15-ppm peak is only about half-dephased; both peaks refocus after 16 cycles (Figure 3). These are typical DRSE results for polycarbonate-like systems.⁹

The Fourier transforms of the time evolution of the 120-ppm protonated aromatic-carbon B signal, and the 15-ppm methyl-carbon T signal, resulted in dipolar sideband spectra (not shown), from which relative intensities for the ratios of the second to first spinning sidebands were determined. The observed aromatic-carbon *n*₂/*n*₁ for the copolymers range from 0.46 ± 0.02 for B₉T to 0.64 for BT + 6T (Table 1). Dipolar sideband ratios for the BT + 6T blend were obtained by difference spectroscopy (Figure 4) and probably involve somewhat larger errors. The aromatic-carbon *n*₂/*n*₁ is 0.55 for BT compared to 0.45 for pure B and 0.45 for the B + T homogeneous blend.

Table 1. Dipolar Rotational Spin-Echo Sideband Intensity Ratios for Copolymers and Blends of Polycarbonate and Tetramethyl Polycarbonate

polymer			dipolar sideband ratio ^a (n_2/n_1)			percent B rings not flipping ^b	
code	mole fraction T	T_g^c (°C)	120-ppm aromatic (B)	30-ppm methyl (B, T)	15-ppm methyl (T)	obsrvd ^d	calcd ^e
B	0	149	0.45	0.42		0	0
B ₉ T	1/10	160	0.46	0.43	0.47	1	1
B ₇ T	1/8	162	0.47	0.42	0.42	2	2
B ₅ T	1/6	161	0.48	0.42	0.40	4	3
B ₃ T	1/4	163	0.53	0.41	0.43	9	6
BT	1/2	174	0.55	0.40	0.43	12	13
BT (aged) ^f	1/2	174	0.58	0.45	0.44	15	13
BT + 6T ^g	7/8	197 ^h	0.64		0.46	22	22
T	1	203		0.47	0.46		

^a Using 0–16 MREV-8 cycles in one rotor period with magic-angle spinning at 1859 Hz. Estimated accuracy (based on signal-to-noise ratios) is ± 0.02 . ^b At a rate greater than 10 kHz at 300 K. ^c From 1-Hz DMS. ^d From 120-ppm aromatic n_2/n_1 . ^e From mole fraction T, and fraction of B rings with intrachain T nearest or next-nearest neighbors (see the Discussion section). ^f At $T > T_g$ (20 h at 180 °C; oven-cooled to room temperature in 2 h). ^g Homogeneous blend of one part BT and six parts T. ^h Estimated.

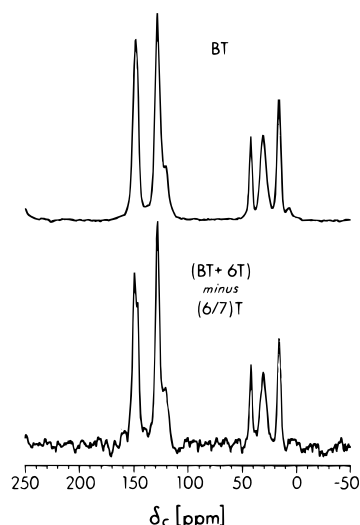


Figure 4. Cross-polarization magic-angle spinning 15.1-MHz ^{13}C NMR spectrum of BT (top). The spectrum at the bottom of the figure was the result of subtracting from the spectrum of a homogeneous blend of one part BT and six parts T the spectrum of a tetramethylpolycarbonate homopolymer, the latter scaled by a factor of six-sevenths.

While the ring methyl-carbon peak at 15 ppm characterizes T ring motion, the methyl-carbon isopropylidene peak at 30 ppm is sensitive to small-amplitude motions of B units in the main chain.²¹ The DRSE dephasing of the two methyl-carbon peaks is similar (Figure 3). The methyl-carbon n_2/n_1 ratios are essentially the same for B, T, all B_xT copolymers, and the BT + 6T blend (Table 1). This was also true in DRSE experiments using two evolution cycles,¹⁶ each with 0–16 MREV-8 cycles per rotor period and magic-angle spinning at 1859 Hz. The methyl-carbon centerband and first and second relative dipolar sideband intensities were 1.5, 1.0, and 0.45 ± 0.02 , respectively, in all cases.

The aromatic-carbon T_1 relaxation behavior⁹ of the 120-ppm peak of BT is slower, particularly for longer evolution times, than that of either B + T or pure B (Figure 5).

Discussion

Fractions of Flipping B and T Rings. In polycarbonate, the protonated aromatic-carbon dipolar sideband n_2/n_1 ratio is 0.45. This value is mostly, but not exclusively, the result⁹ of averaging of the ^1H – ^{13}C dipolar coupling by ring-flip rates greater than about

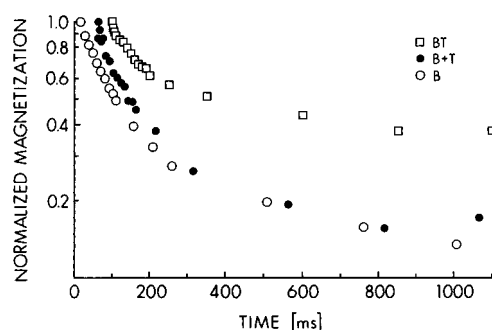


Figure 5. ^{13}C spin-lattice relaxation behavior of the 120-ppm aromatic-carbon peak of (i) polycarbonate homopolymer (open circles); (ii) a homogeneous blend of one part polycarbonate and one part tetramethylpolycarbonate (closed circles) and BT polycarbonate copolymer (open squares). The latter two data sets have been displayed horizontally for clarity.

10 kHz at 300 K. In the absence of large-amplitude motional averaging, n_2/n_1 is 1.3. We determine the fraction, f , of B phenylene rings that are flipping in B_xT from $(n_2/n_1)_{\text{obsrvd}} = 0.45f + 1.3(1 - f)$, where the observed sideband ratio corresponds to the 120-ppm aromatic-carbon peak, which arises exclusively from B units. Because the observed ratios are all close to 1/2 (Table 1), most of the B rings are flipping, even in copolymers with high concentrations of T. The fraction of B rings not flipping, $1 - f$, is reported in Table 1. For the BT + 6T homogeneous blend, 22% of the B rings are not flipping and 78% are flipping. On the basis of a compositional extrapolation, we estimate that, in the limit that single B units of BT blends are completely surrounded by T, about 75% of the B rings would still be flipping.

While most of the B rings are flipping in B_xT, none of the T rings are. The methyl-carbon n_2/n_1 for the ring and main chain are indistinguishable (Table 1). A flipping T ring would have had its 15-ppm methyl-carbon n_2/n_1 reduced by half relative to that for the main chain.⁹

Ring Dynamics and Interchain Packing. Even though all of the B rings in B + T are flipping ($n_2/n_1 = 0.45$), only 88% in BT are flipping ($n_2/n_1 = 0.55$). Thus, the increased stiffness of the BT main chain (resulting from increased steric hindrance of the ring methyls, not from a change in flexibility of the carbonate linkage) is an ingredient in stopping 12% of the B rings from flipping (Table 1). However, it cannot be the only ingredient. That is, if all the B units that had intrachain T nearest neighbors were constrained, then all

the B rings of BT would be nonflippers, instead of only 12% of them. We conclude that interchain packing¹⁵ in B_xT must contribute to stopping B-ring flips, even though no B rings are stopped from flipping in homogeneous blends of pure B with pure T. (At least no B rings are blocked in B + T; we have recently determined that 6% of the B rings are blocked in a homogeneous blend of one part specifically ¹³C-labeled B with 19 parts T. These experiments will be described in this journal in detail later.)

Naturally, the stiffness of a B unit proximate to a T unit within a B_xT chain diminishes as the length of the B run increases. If we assume that the increased stiffness persists only for nearest and next-nearest neighbors to T units, then all the B units in BT and B₃T would be affected, four-fifths in B₅T, four-sevenths in B₇T, and so on. With this assumption, we can account for the fraction of B rings not flipping in B_xT by a simple product of three terms: (i) the estimated upper limit of 25% for constrained B rings of BT completely surrounded by T; (ii) the fraction of B units affected by an intrachain T-induced stiffness (just described); and (iii) the mole fraction of T. For example, the calculated fraction of B rings not flipping in pure BT is $\frac{1}{4} \times 1 \times \frac{1}{2} = \frac{1}{8} = 0.12$. Similar calculations for all the B_xT copolymers are presented in Table 1 (last column) and are in good agreement with the observed fractions of B rings not flipping. The simplicity of this accounting supports the notion that there is a *single* nearest-neighbor chain that is dominant in determining the ring dynamics of any chain in polycarbonate glasses. In the B_xT system, this dominant nearest-neighbor chain apparently must present a T ring proximate to a B ring to stop the B ring from flipping, which explains the *linear* dependence of the fraction of nonflipping rings on the mole fraction of T in the copolymer.

Whitney–Yaris Model for Ring Flips in Polycarbonate. Whitney and Yaris²² have developed a generalized Langevin dynamics simulation of motion for a model of pure polycarbonate and have suggested a possibility for the mechanism of the ring-flipping process. A phenylene-ring π flip occurs when there is an increase of about 0.5 Å in the separation between the center of a ring and that of the closest ring of the nearest-neighbor chain. This nearest-neighbor pair are part of a bundle of chains, which is a small collection of chains, the directions of whose main chains are locally parallel.²³ The separation between nearest-neighbor rings must be accompanied by an increase in the rotational kinetic energy of the ring attempting the flip. In the Whitney–Yaris model, the π -flip gate in polycarbonate results from the synchronization of the arrival of a lattice phonon with a reduction in an intermolecular steric barrier. The lattice dilation within the bundle is mechanically active.

Because of the structural similarity and complete miscibility^{15,20} of B, T, and B_xT, it seems reasonable to suppose that the Whitney–Yaris model is applicable to the blends and copolymers of B and T, as well as to B itself. Within the framework of the Whitney–Yaris model, no T ring can ever flip faster than 10 kHz at 300 K because the 0.5-Å reductions in inter-ring separations do not lower the barriers sufficiently for 180° rotations of methyl-substituted rings. Furthermore, no B ring in a B + T blend is ever constrained from flipping because a 20° rotation about the T-ring C₂ axis is sufficient to move the methyl group out of the way of a flipping ring. (Such ring fluctuations are always present.)²² On the

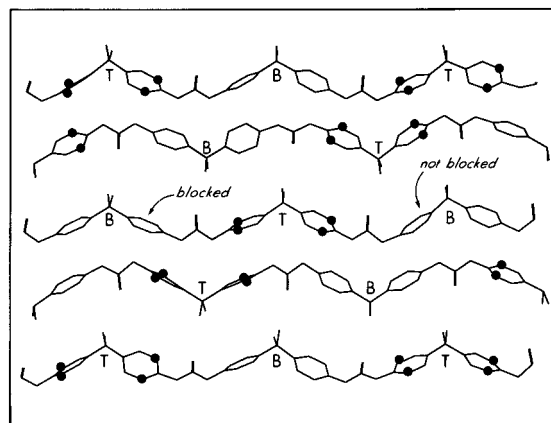


Figure 6. Slice through a Whitney–Yaris bundle of chains for a BT completely alternating polycarbonate copolymer. Solid circles represent ring methyl groups. For the central chain, one of the nonmethylated rings on the left has a methylated ring for a nearest neighbor. In addition, this B ring is in a part of the chain locally stiffened by an interchain interaction between two T rings. The stiffened chain has a reduced ability to rearrange cooperatively with its neighbors. Thus, the B ring on the left is blocked from flipping by a combination of interchain steric interactions that are absent for the B ring on the right.

other hand, it is plausible that the increased stiffness (steric drag) of B units near T units in B_xT would be sufficient to enable a proximate T ring to block a B-ring flip, at least in a fraction of sites in the glass. By this interpretation, the 12% fraction of nonflipping B rings in pure BT is due to the most densely packed regions in the glass.

Figure 6 shows a slice through a Whitney–Yaris bundle of BT chains. For the central chain, one of the nonmethylated rings on the left has a methylated ring for a nearest neighbor. In addition, this B ring is in a part of the chain that is stiffened by interchain interactions of two methylated rings. The stiffened chain has a reduced ability to rearrange cooperatively with its neighbors and so provide the 0.5-Å dilation needed for the B ring on the left to flip. Thus, this particular ring is blocked by a *combination* of interchain steric interactions. The B ring on the right of the same chain, on the other hand, has neither interaction and is free to flip. The net result is that, for BT chains, some B rings flip and some do not.

Macroscopic Relaxation in B_xT. The reduction of the $T = -100$ °C γ transition and increase of DMS lossiness near $T = -20$ °C for BT and B₃T relative to those for B₇T and B₉T (Figure 1) indicate a stiffening of the B_xT lattice with increasing T content. The stiffening is due to interchain steric repulsions associated with the ring methyl groups (*cf.* above). In tetramethylpolycarbonate homopolymer both the $T = -100$ and $T = -20$ °C transitions are completely gone.¹⁵ The increase in stiffness and decrease in flexibility with increasing T content measured by DMS are consistent with the observed decrease in protonated aromatic-carbon NMR spin–lattice relaxation for BT relative to pure polycarbonate (Figure 5). The slower NMR relaxation means that the average rates of cooperative ring flips and wiggles have been reduced⁹ although neither has been eliminated.

Despite the similarities in DMS and NMR measures of stiffness, a low concentration of T in B_xT has a more pronounced effect on DMS relaxation than on NMR DRSE behavior. For example, the DMS of B₉T still has a significant loss peak at $T = -20$ °C (Figure 1), much

greater than might be anticipated from the composition of the copolymer, whereas the ^{13}C DRSE relaxation behavior of B_9T is virtually indistinguishable from that of B with a little T mixed in (Table 1). We attribute this qualitative difference in behavior to the sensitivity of DMS to a generally larger physical domain. We have shown before¹⁰ that even the γ -relaxation DMS peak (at 0.01 Hz) of polycarbonate has two components, one associated with intrabundle motions and one with interbundle motions. (As mentioned above, the term "bundle" refers to a collection of chains with approximately the same local orientational order.) The interbundle motion requires cooperativity over a larger region than the intrabundle motion and so takes place at a slower rate. The cooperative movement of many chains is necessary to generate a lattice dilation sufficient to enable T-ring large-amplitude motion.²² Thus, the DMS relaxation at $T = -20^\circ\text{C}$ is necessarily a large-volume process in B_xT , and the larger the volume over which the motion occurs, the more important the effect of low concentrations of T. (Polycarbonate has no DMS relaxation at $T = -20^\circ\text{C}$ because motions on the spatial scale required for this transition are macroscopically phase incoherent, which is due to the local chain flexibility present in polycarbonate but absent in B_xT .) The NMR-detected B-ring flips in B_xT , on the other hand, depend on the packing of only pairs of chains, and so there is no spatial long-range influence of T content on the NMR DRSE behavior.

Acknowledgment. This work was supported by NSF Grant DMR-9015864 (J.S.).

References and Notes

- (1) Struik, L. C. E. *Physical Aging of Amorphous Polymers and Other Materials*; Elsevier: Amsterdam, The Netherlands, 1978.
- (2) Wu, J. Thesis, The University of Michigan, Ann Arbor, MI, 1997.
- (3) Heijboer, J. In *Molecular Basis of Transitions and Relaxations*; Meier, D. J., Ed.; Gordon and Breach: New York, 1978; pp 75–102.
- (4) Yee, A. F.; Smith, S. A. *Macromolecules* **1981**, *14*, 54.
- (5) Skolnick, J.; Perchak, D.; Yaris, R.; Schaefer, J. *Macromolecules* **1984**, *17*, 2332.
- (6) Schaefer, J.; Stejskal, E. O.; Perchak, D.; Skolnick, J.; Yaris, R. *Macromolecules* **1985**, *18*, 368.
- (7) Spiess, H. W. *Colloid Polym. Sci.* **1983**, *261*, 193.
- (8) O'Gara, J. F.; Desjardins, S. G.; Jones, A. A. *Macromolecules* **1981**, *14*, 64.
- (9) Schaefer, J.; Stejskal, E. O.; McKay, R. A.; Dixon, W. T. *Macromolecules* **1984**, *17*, 1479.
- (10) Lee, P. L.; Kowalewski, T.; Poliks, M. D.; Schaefer, J. *Macromolecules* **1995**, *28*, 2476.
- (11) Walton, J. H.; Lizak, M. J.; Conradi, M. S.; Gullion, T.; Schaefer, J. *Macromolecules* **1990**, *23*, 416.
- (12) Hansen, M. T.; Boeffel, C.; Spiess, H. W. *Colloid Polym. Sci.* **1993**, *271*, 446.
- (13) Xiao, C.; Yee, A. F. *Macromolecules* **1992**, *25*, 6800.
- (14) Schmidt, A.; Kowalewski, T.; Schaefer, J. *Macromolecules* **1993**, *26*, 1729.
- (15) Jho, J. Y.; Yee, A. F. *Macromolecules* **1991**, *24*, 1905.
- (16) Bork, V.; Gullion, T.; Hing, A.; Schaefer, J. *J. Magn. Reson.* **1990**, *88*, 523.
- (17) Rhim, W. K.; Elleman, D. D.; Vaughan, R. W. *J. Chem. Phys.* **1973**, *59*, 3740.
- (18) Garbow, J. R.; Schaefer, J. *Macromolecules* **1987**, *20*, 819.
- (19) Schaefer, J.; McKay, R. A.; Stejskal, E. O.; Dixon, W. T. *J. Magn. Reson.* **1983**, *52*, 123.
- (20) Fischer, E. W.; Hellmann, G. P.; Spiess, H. W.; Hörth, F. J.; Ecarius, U.; Wehrle, M. *Makromol. Chem. Suppl.* **1985**, *12*, 189.
- (21) Lee, P. L.; Schaefer, J. *Macromolecules* **1995**, *28*, 2577.
- (22) Whitney, D.; Yaris, R. *Macromolecules* **1997**, *30*, 1741.
- (23) Klug, C. A.; Zhu, W.; Tasaki, K.; Schaefer, J. *Macromolecules* **1997**, *30*, 1734.

MA970630U